



A compressibility correction of the pressure strain correlation model in turbulent flow

Hechmi Klifi*, Taieb Lili

Département de physique, faculté des sciences de Tunis, campus universitaire, 1060, Tunis, Tunisia

ARTICLE INFO

Article history:

Received 31 March 2012

Accepted after revision 8 April 2013

Available online 2 May 2013

Keywords:

Turbulence
Compressible
Pressure strain
Homogeneous
Mixing layers

ABSTRACT

This paper is devoted to the second-order closure for compressible turbulent flows with special attention paid to modeling the pressure–strain correlation appearing in the Reynolds stress equation. This term appears as the main one responsible for the changes of the turbulence structures that arise from structural compressibility effects. From the analysis and DNS results of Simone et al. and Sarkar, the compressibility effects on the homogeneous turbulence shear flow are parameterized by the gradient Mach number. Several experiment and DNS results suggest that the convective Mach number is appropriate to study the compressibility effects on the mixing layers. The extension of the LRR model recently proposed by Marzougui, Khlifi and Lili for the pressure–strain correlation gives results that are in disagreement with the DNS results of Sarkar for high-speed shear flows. This extension is revised to derive a turbulence model for the pressure–strain correlation in which the compressibility is included in the turbulent Mach number, the gradient Mach number and then the convective Mach number. The behavior of the proposed model is compared to the compressible model of Adumitroaie et al. for the pressure–strain correlation in two turbulent compressible flows: homogeneous shear flow and mixing layers. In compressible homogeneous shear flows, the predicted results are compared with the DNS data of Simone et al. and those of Sarkar. For low compressibility, the two compressible models are similar, but they become substantially different at high compressibilities. The proposed model shows good agreement with all cases of DNS results. Those of Adumitroaie et al. do not reflect any effect of a change in the initial value of the gradient Mach number on the Reynolds stress anisotropy. The models are used to simulate compressible mixing layers. Comparison of our predictions with those of Adumitroaie et al. and with the experimental results of Goebel et al. shows good qualitative agreement.

© 2013 Académie des sciences. Published by Elsevier Masson SAS. All rights reserved.

1. Introduction

Compressibility effects on turbulence are a challenging problem for environmental and aeronautical applications. Understanding better compressibility effects on high-speed mixing layers is highly relevant in terms of engineering importance. It is well known that the growth rate of turbulence mixing layers thickness is substantially reduced with increasing the convective Mach number. The compressibility phenomena have been studied extensively and numerical simulation of compressible turbulent flows using compressible turbulence models have been performed by many authors. Previous studies carried out in the last 20 years conjectured that compressibility effect was linked with dilatational dissipation and pressure–dilatation correlation, as it is represented by the models of Zeman [1], Sarkar [2] and others. According to the DNS results of Simone

* Corresponding author.

E-mail address: khlfihachmi@yahoo.fr (H. Klifi).

et al. [3] and Sarkar [4], the dilatational terms have a negligible contribution to the changes of the compressible turbulence structure. Hamba [5] have performed DNS measurements of compressible homogeneous shear flows and reached similar conclusions about the roles of dilatational terms. These conclusions are confirmed by Vreman et al. [6] and Pantano and Sarkar [7] in their DNS results, which show that the dilatational terms do not affect the compressible mixing layers. On the other hand, all of these findings indicate that compressibility effects on pressure play a principal role. It is concluded that reduced pressure fluctuations and then reduction of pressure–strain correlation are the main ones responsible for the dramatic changes in the magnitude of Reynolds stress anisotropies. It was observed from the DNS results of Simone et al. [3] and of Sarkar [4] regarding compressible homogeneous shear flows that there are some important physical discrepancies: a dramatic increase in normal Reynolds stress anisotropies, a significant decrease in the Reynolds shear stress anisotropy and a decrease in the growth rate of the turbulent kinetic energy with increasing the gradient Mach number, which is defined by $M_g = Sl/\bar{a}$, where \bar{a} is the mean speed of sound and l is the length scale of energetic turbulence motions; this number is also interpreted as the ratio between the acoustic time scale $T_a = l/\bar{a}$ and the mean distortion time scale $T_d = 1/S$, where $S = \sqrt{\tilde{U}_{i,j}\tilde{U}_{j,i}}$ and $M_g = T_a/T_d$. Also, in the DNS of Simone et al. [3], it can be seen that there is an amplification of the turbulent kinetic energy with increasing the gradient Mach number at low St ($St < 5$), for $St > 5$, whereas trend change and compressibility tend to stabilize turbulent shear flows. These discrepancies from which the compressibility appear to be related to the gradient Mach number are found in DNS results [4,3], in which one can see that after an initial slight increase with St ($St < 5$), M_g shows a trend towards becoming asymptotically constant, contrary to the turbulent Mach number M_t ($M_t = \sqrt{2K}/\bar{a}$, where $K = \overline{u'_i u'_i}/2$ is the turbulent kinetic energy and \bar{a} is the mean speed of sound), which grows constantly with St . Obviously, the structure of M_g is similar to that of turbulence. As a consequence of this, M_g seems to be an appropriate parameter to study structural compressibility effects, and it may be useful to establish compressible turbulence models that are indispensable for a precise simulation of high shear flows. More recently, a M_t -corrected form of the Launder, Reece and Rodi model for the pressure–strain correlation has been proposed by Marzougui, Khlifi and Lili [8]. Applications of this model on compressible homogeneous shear flows have shown a qualitative agreement with the DNS results of Sarkar [4] for cases A_1 , A_2 , and A_3 , which correspond to moderate mean shear. Conversely, in case A_4 , the predictions model [8] is in disagreement with DNS results [4]. In this study, we revised the extension of the LRR model [9] proposed by Marzougui, Khlifi and Lili [8] to derive a model for the pressure–strain correlation in which the gradient Mach number and the convective Mach number are used with the turbulent Mach number to express compressibility effects. It is observed from several experiment and DNS results of compressible mixing layers that the Reynolds stresses decrease with the increased convective Mach number M_c ; this number is defined by $M_c = \frac{\bar{U}_1 - \bar{U}_2}{\bar{a}_1 + \bar{a}_2}$, subscript 1 denotes the value of the upper stream, while subscript 2 denotes the value of the lower stream. These results suggest that some of the physical properties of the compressible mixing layers are clearly visible if compressibility effects are related to the convective Mach number. In accordance with the concept allowing for the compressible mixing layer which is well related to the homogeneous shear flow, M_c is connected to M_g (see Sarkar [4]). Thus, the convective Mach number is involved in the proposed model for the pressure–strain correlation. The ability of the proposed model to predict the fully developed turbulent compressible homogeneous shear flow and mixing layers is examined in different cases from DNS data [4,3] and experiments by Goebel and Dutton [10]. Our predictions are compared to those obtained by the compressible model of Adumitroaie et al. [11].

2. Governing equations

The general equations governing the motion of a compressible fluid are the Navier–Stokes equations. They can be written as follows for mass, momentum and energy conservation:

$$\frac{\partial}{\partial t}\rho + \frac{\partial}{\partial x_i}\rho u_i = 0 \quad (1)$$

$$\frac{\partial}{\partial t}\rho u_i + \frac{\partial}{\partial x_j}\rho u_i u_j = \frac{\partial}{\partial x_j}\sigma_{ij} \quad (2)$$

$$\frac{\partial}{\partial t}\rho e + \frac{\partial}{\partial x_j}\rho e u_j = \frac{\partial}{\partial x_j}\sigma_{ij} u_i - \frac{\partial}{\partial x_j}(\kappa T_j) \quad (3)$$

Here ρ is the density, u is the velocity, p is the pressure, e is the internal energy, T is the temperature, μ is the viscosity, κ is the thermal conductivity and c_v is specific heat at constant volume.

$$e = c_v T, \quad \sigma_{ij} = -p\delta_{ij} + \tau_{ij}, \quad \tau_{ij} = 2\mu S_{ij}, \quad S_{ij} = (u_{i,j} + u_{j,i})/2$$

For an ideal gas, the relation between pressure, density and temperature can be written as follows:

$$p = \rho RT \quad (4)$$

2.1. Basic equations of the Favre second-order closure in compressible flows

The Favre equations for conservation of mass, momentum and energy are:

$$\frac{\partial}{\partial t} \bar{\rho} + \frac{\partial}{\partial x_i} (\bar{\rho} \tilde{U}_i) = 0 \tag{5}$$

$$\frac{\partial}{\partial t} (\bar{\rho} \tilde{U}_i) + \frac{\partial}{\partial x_j} (\bar{\rho} \tilde{U}_i \tilde{U}_j) + \frac{\partial}{\partial x_j} (\overline{\rho u''_i u''_j}) = \frac{\partial}{\partial x_j} [\tilde{\tau}_{ij} + \overline{\tau''_{ij}} - \bar{p} \delta_{ij}] \tag{6}$$

$$\frac{\partial}{\partial t} (\bar{\rho} \tilde{C}_v \tilde{T}) + \frac{\partial}{\partial x_i} (\bar{\rho} \tilde{C}_v \tilde{T} \tilde{U}_i) = -\bar{p} \frac{\partial}{\partial x_i} \tilde{U}_i - \bar{p} \frac{\partial}{\partial x_i} \overline{u''_i} - \overline{p' \frac{\partial}{\partial x_i} u''_i} + \bar{\Phi} + \frac{\partial}{\partial x_i} \left(\kappa \frac{\partial}{\partial x_i} \overline{T} \right) - \frac{\partial}{\partial x_i} (\bar{\rho} C_v \overline{u''_i T''}) \tag{7}$$

where

$$\tilde{\tau}_{ij} = 2\bar{\mu} \tilde{S}_{ij} - \frac{2}{3} \bar{\mu} \tilde{U}_{k,k} \delta_{ij}$$

$$\tilde{S}_{ij} = (\tilde{U}_{i,j} + \tilde{U}_{j,i})/2$$

$$\tau''_{ij} = 2\bar{\mu} s''_{i,j} - \frac{2}{3} \bar{\mu} u''_{k,k} \delta_{ij}$$

$$\bar{\Phi} = \overline{\tau_{ij} u_{ij}}$$

The Reynolds stress are solutions of the transport equation, namely:

$$\frac{\partial}{\partial t} (\bar{\rho} \overline{u''_i u''_j}) + \frac{\partial}{\partial x_m} (\bar{\rho} \overline{u''_i u''_j} \tilde{U}_m) = P_{ij} + D_{ijm,m} + \phi_{ij} + \epsilon_{ij} + V_{ij} \tag{8}$$

where the terms P_{ij} , D_{ijm} , ϕ_{ij} , ϵ_{ij} and V_{ij} are:

$$P_{ij} = -(\bar{\rho} \overline{u''_i u''_m} \tilde{U}_{j,m} + \bar{\rho} \overline{u''_j u''_m} \tilde{U}_{i,m})$$

$$D_{ijm} = -(\bar{\rho} \overline{u''_i u''_j u''_m} + \overline{p' u''_j} \delta_{im} + \overline{p' u''_i} \delta_{jm} - \overline{\tau''_{im} u''_j} - \overline{\tau''_{jm} u''_i})$$

$$\phi_{ij} = 2\overline{p' (u''_{i,j} + u''_{j,i})}$$

$$\epsilon_{ij} = -\overline{\tau''_{im} u''_{j,m}} - \overline{\tau''_{jm} u''_{i,m}}$$

$$V_{ij} = -\bar{p}_{,j} \overline{u''_i} - \bar{p}_{,i} \overline{u''_j} + \tilde{\tau}_{im,m} \overline{u''_i} + \tilde{\tau}_{jm,m} \overline{u''_j}$$

Classically, the second-order closure suggests to determine the dissipation term ϵ_{ij} by using the isotropic dissipation model:

$$\epsilon_{ij} = \frac{2}{3} \epsilon \delta_{ij} \tag{9}$$

A concept of the dilatational dissipation was proposed by Zeman [1] and Sarkar [2] as:

$$\epsilon = \epsilon_s + \epsilon_c \tag{10}$$

where $\epsilon_s = \overline{\bar{\nu} \omega_i \omega_j}$, ω_i is the fluctuating vorticity and $\epsilon_c = \frac{4}{3} \overline{\bar{\nu} u_{i,i}^2}$ denote the solenoidal and dilatational parts of the turbulent dissipation respectively. The authors argued that the solenoidal part of the dissipation can be modeled by using the traditional incompressible equation model and ϵ_c is determined by the commonly used model [1,2] as:

$$\epsilon_c = g_c \epsilon_s \tag{11}$$

g_c is a function of the turbulent Mach number, according to [2], $g_c = 0.5M_t^2$. From above, the total turbulent dissipation rate is written as:

$$\epsilon = (1 + 0.5M_t^2) \epsilon_s \tag{12}$$

3. The compressible turbulence models

Many DNS and experimental studies have been carried out on compressible turbulent flows, most of which show significant compressibility effects on the pressure–strain correlation via pressure fields. Such effects induce reduction in the magnitude of the anisotropy of the Reynolds shear stress and increase in the magnitude of the normal stress anisotropy. Consequently, the pressure–strain correlation requires a careful modeling in the Reynolds stress turbulence model. With respect to the incompressible case, many compressible models have been developed for the pressure–strain correlation. Hereafter, most of all these models are generated from a simple extension of its incompressible counterpart; they perform well in the simulation of important turbulent flows evolving with moderate compressibility. Adumitroaie et al. [11] assumed that an incompressible modeling approach of the pressure strain can be used to develop turbulent models taking into account compressibility effects. Considering a non-zero divergence for the velocity fluctuations called the compressibility continuity constraint and using different models for the pressure dilatation, which is proportional to the trace of the pressure strain, their model for the pressure strain is written as:

$$\begin{aligned} \Phi_{ij}^* = & -C_1 \bar{\rho} \varepsilon_s b_{ij} + \left(\frac{4}{5} + \frac{2}{5} d_1 \right) \bar{\rho} K \left(\tilde{S}_{ij} - \frac{1}{3} \tilde{S}_{ll} \delta_{ij} \right) + 2 \bar{\rho} k (1 - C_3 + 2d_2) \left[b_{ik} \tilde{S}_{jk} + b_{jk} \tilde{S}_{ik} - \frac{2}{3} b_{ml} \tilde{S}_{ml} \delta_{ij} \right] \\ & - \bar{\rho} k (1 - C_4 - 2d_2) \left[b_{ik} \tilde{\mathcal{D}}_{jk} + b_{jk} \tilde{\mathcal{D}}_{ik} - \frac{4}{3} d_2 b_{ij} \tilde{S}_{kk} \right] \end{aligned} \quad (13)$$

where $\tilde{S}_{i,j} = 0.5(\tilde{U}_{i,j} + \tilde{U}_{j,i})$, $\tilde{\mathcal{D}}_{i,j} = 0.5(\tilde{U}_{i,j} - \tilde{U}_{j,i})$ and $b_{ij} = \widehat{u_i'' u_j''} - 2/3 K \delta_{ij}$.

The compressibility coefficients d_1 and d_2 are determined from some compressible closures for the pressure–dilatation correlation.

Regarding the influence of the pressure strain on the behaviors of the Reynolds stress, different analysis have also been carried out for this term. Fujihiro et al. [5] discuss this question within the context of a compressible homogeneous shear flow. To show how the pressure–strain correlation reduces the growth rate of the turbulent kinetic energy, they focused their analysis on the pressure–strain component Π_{22} and they deduced that this term appears as the first cause in the dramatic changes of the turbulence, which are due to structural compressibility effects. In fact, when Π_{22} is reduced, this causes a reduction in R_{22} , which in turn affects Π_{12} . Indeed, Π_{12} causes a reduction in the magnitude of R_{12} , Π_{11} and the growth rate of the turbulent kinetic energy. As a consequence, the authors suggest that the modifications of C_3 and C_4 that affect directly Π_{22} appear as sufficient to capture the coherent structural compressibility effects. In this context, the results of C.H. Park and S.O. Park [12] show that in addition to the modifications of C_3 and C_4 , coefficient C_2 should be modified. In fact, this coefficient affects the shear pressure–strain component (Π_{12}), which has an evident importance in the transport equation for the shear Reynolds stress. This is the preferred focal point of our modeling strategy for the pressure–strain correlation and from which we revise the proposed extension of LRR model [8].

$$\begin{aligned} \Phi_{ij}^* = & -C_1 \bar{\rho} \varepsilon_s b_{ij} + C_2 \bar{\rho} k \left(\tilde{S}_{ij} - \frac{1}{3} \tilde{S}_{ll} \delta_{ij} \right) + C_3 \bar{\rho} k \left(b_{ik} \tilde{S}_{jk} + a_{jk} \tilde{S}_{ik} - \frac{2}{3} b_{ml} \tilde{S}_{ml} \delta_{ij} \right) \\ & + C_4 \bar{\rho} k (b_{ik} \tilde{\mathcal{D}}_{jk} + b_{jk} \tilde{\mathcal{D}}_{ik}) \end{aligned} \quad (14)$$

where

$$C_1 = \frac{C_1^I}{(1 + 0.5M_t^2)} (1 - 0.44M_t^2)^2$$

$$C_2 = C_2^I = 0.8$$

$$C_3 = C_3^I (1 - 1.5M_t^2)$$

$$C_4 = C_4^I (1 - 0.5M_t)$$

The coefficients C_i^I are those of the LRR model [9]: $C_1^I = 3$, $C_2^I = 0.8$, $C_3^I = 1.75$, $C_4^I = 1.31$.

3.1. A modification of the C_2 -coefficient in Marzougui, Khlifi and Lili's model [8]

In Marzougui, Khlifi and Lili's model [8], one can see that coefficient C_2 is taken as in the incompressible model. To modify this coefficient appearing in the shear pressure–strain component Π_{12} , we consider the equation for the fluctuating dilatation $d' = u'_{i,i}$ as in [13], namely:

$$\begin{aligned} \frac{d}{dt} d' = & -2 \frac{\partial u'_j}{\partial x_i} \frac{\partial U_i}{\partial x_j} - \frac{\partial u'_i}{\partial x_j} \frac{\partial u'_j}{\partial x_i} + \frac{\rho'}{\bar{\rho}^2} \frac{\partial^2 \bar{p}}{\partial x_i^2} \\ & + \frac{1}{\bar{\rho}^2} \frac{\partial \rho'}{\partial x_i} \frac{\partial \bar{p}}{\partial x_i} + \frac{1}{\bar{\rho}^2} \frac{\partial p'}{\partial x_i} \frac{\partial \bar{\rho}}{\partial x_i} - 2 \frac{\rho'}{\bar{\rho}^2} \frac{\partial \bar{\rho}}{\partial x_i} \frac{\partial \bar{p}}{\partial x_i} - \frac{1}{\bar{\rho}} \frac{\partial^2 p'}{\partial x_i^2} + \frac{4}{3} \nu \frac{\partial^2 d'}{\partial x_i^2} \end{aligned} \quad (15)$$

Multiplying both sides by p' and taking the ensemble averaging, we therefore write this equation as follow:

$$\overline{p' \frac{d}{dt}} = -2 \overline{p' \frac{\partial u'_j}{\partial x_i} \frac{\partial \bar{U}_i}{\partial x_j}} + \dots \tag{16}$$

Generally, the mean shear effects arising essentially from the mean velocity gradient are important in compressible shear flow, the other terms in Eq. (16) are considered as negligible, so we can write:

$$\frac{\overline{p'd'}}{\tau} = -2 \overline{p' \frac{\partial u'_j}{\partial x_i} \frac{\partial \bar{U}_i}{\partial x_j}} \tag{17}$$

where τ is the characteristic time scale of the dilatation fluctuations [1], $\tau = \alpha M_t^2 K / \varepsilon$. Also, this equation can be written as:

$$\frac{\overline{p'd'}}{\tau} = -2 \left(\overline{p' \frac{\partial u'_j}{\partial x_i}} \right)^* \frac{\partial \bar{U}_i}{\partial x_j} - \frac{2}{3} \overline{p'd'} \frac{\partial \bar{U}_i}{\partial x_i} \tag{18}$$

where $\left(\overline{p' \frac{\partial u'_j}{\partial x_i}} \right)^* = \overline{p' \frac{\partial u'_j}{\partial x_i}} - \frac{1}{3} \overline{p'd'} \delta_{ij}$ is the deviatoric part of the pressure–strain correlation.

According to the isotropization of the production, only the mean velocity gradient term in the linear pressure–strain part is considered here, and we can write:

$$\left(\overline{p'u'_{i,j}} \right)^* = -C_1 \bar{\rho} \varepsilon_s b_{ij} + C_2 \bar{\rho} K \tilde{S}_{ij}^* \tag{19}$$

where $\tilde{S}_{ij}^* = \tilde{S}_{ij} - \frac{1}{3} \tilde{S}_{ll} \delta_{ij}$.

It is well known that there are some compressible models for the pressure–strain correlation. In this study, we choose the Marzougui, Khlifi and Lili’s model [8] to deduce an expression for $\left(\overline{p'u'_{i,j}} \right)^*$ as:

$$\left(\overline{p'u'_{i,j}} \right)^* = f(M_t) \bar{\rho} \varepsilon_s b_{ij} + C_2 \bar{\rho} K S_{ij}^* \tag{20}$$

where $f(M_t)$ is a function of the turbulent Mach number:

$$f(M_t) = -C_1^l \frac{1 + \beta_1 M_t^4 - \beta_2 M_t^2}{1 + 0.5 M_t^2} \tag{21}$$

The model coefficients β_1 and β_2 are positive. The coefficient C_1^l is constant ($C_1^l = 3$ in the LRR model [9]), thus, function $f(M_t)$ preserves in the limit case ($M_t = 0$) the universality of the standard model. Thus, Eq. (18) takes the form:

$$\overline{p'd'} = -2 \bar{\rho} \frac{\alpha M_t^2}{1 + 0.5 M_t^2} \left[f(M_t) K b_{ij} + C_2 \frac{K^2}{\varepsilon_s} S_{ij}^* \right] \bar{U}_{i,j} - \frac{2}{3} \frac{K}{\varepsilon_s} \overline{p'd'} \delta_{ij} \tag{22}$$

According to the Sarkar et al.’s model [2], $\overline{p'd'}$ can be written as:

$$\overline{p'd'} = f_c \bar{\rho} K b_{ij} \bar{U}_{i,j} + \dots \tag{23}$$

The compressible function is proportional to the turbulent Mach number:

$$f_c = \beta_3 M_t^2 \tag{24}$$

Substituting $\overline{p'd'}$ by its expression in Eq. (23) and using identification between terms that affect the mean gradient velocity, one can find easily that the turbulent production $P = -\overline{u'_i u'_j \bar{U}_{i,j}}$ verifies the following relation:

$$P = -\frac{2}{3} K \bar{U}_{l,l} + \frac{C_2}{f(M_t) + \frac{f_c}{2\alpha M_t^2} (1 + 0.5 M_t^2)} \frac{K^2}{\varepsilon_s} S_{ij}^* \bar{U}_{i,j} \tag{25}$$

In the framework of the $(K - \varepsilon)$ model, the turbulent viscosity model is used to write the production as follow:

$$P = -\frac{2}{3} K \bar{U}_{l,l} + \nu_t S_{ij}^* \bar{U}_{i,j} \tag{26}$$

where the turbulent viscosity ν_t is defined by:

$$\nu_t = C_\mu \frac{K^2}{\varepsilon_s (1 + 0.5 M_t^2)} \tag{27}$$

coefficient C_μ is a model constant; for an incompressible flow, $C_\mu = 0.09$.

The use of Eqs. (25), (26), (27) lead to the following expression for C_2 :

$$C_2 = \frac{C_\mu}{(1 + 0.5M_t^2)} \left(f(M_t) + \frac{f_c}{2\alpha M_t^2} (1 + 0.5M_t^2) \right) \quad (28)$$

According to the models of Marzougui, Khlifi and Lili [8] and of Sarkar et al. [2] of $f(M_t)$ and f_c , respectively, we obtain:

$$C_2 = C_\mu g(M_t) \quad (29)$$

where $g(M_t)$ is a polynomial compressibility function of the turbulent Mach number, namely:

$$g(M_t) \simeq \frac{-(1 + \beta_1 M_t^4 - \beta_2 M_t^2) + \frac{\beta_3}{2\alpha} (1 + 0.5M_t^2)^2}{(1 + 0.5M_t^2)^2} \quad (30)$$

and then

$$g(M_t) \simeq - \left[(1 + \beta_1 M_t^4 - \beta_2 M_t^2) + \frac{\beta_3}{2\alpha} (1 + 0.5M_t^2)^2 \right] (1 - M_t^2) \quad (31)$$

Regarding the structural compressibility effects on the compressible homogeneous shear flow, Heinz [14] proposed a model for C_μ in the following form:

$$C_\mu = C_{\mu 0} e^{(-\beta M_g)} \quad (32)$$

One can remark that C_μ decreases when M_g increases and that, in the case of an incompressible flow, $C_\mu = C_{\mu 0} \simeq 0.09$.

Examination of the DNS results of Sarkar [4] shows that the shear stress anisotropy is unaffected by compressibility effects for low turbulent Mach numbers. For moderate and high turbulent Mach number, compressibility increases strongly with increasing M_t . Following that, one can deduce that for low M_t s, coefficient C_2 is the same as in the LRR model [9], so the effect of the $g(M_t)$ -compressibility function is negligible. For moderate and high M_t s, the $g(M_t)$ -compressibility function should change quickly to cause the dramatic changes of the pressure-strain correlation with increasing the turbulent Mach number; so we propose for the compressibility function the simplest model, which reads:

$$g(M_t) \propto (1 + \lambda M_t^4) \quad (33)$$

where λ is a constant model.

One can see that the term M_t^4 can ensure the structural changes on the pressure strain between the low- M_t and the high- M_t compressible regimes.

From the above equations, we have for C_2 the following model:

$$C_2 \propto (1 + \lambda M_t^4) c_{\mu 0} \exp(-\beta M_g) \quad (34)$$

It is clear that for incompressible flow M_t and M_g are equal to zero and the coefficient C_2 coincides with its incompressible homolog C_2^I involved in LRR model [9], this allows to write:

$$C_2 = C_2^I (1 + \lambda M_t^4) e^{(-\beta M_g)} \quad (35)$$

The calibration of β and λ based on direct numerical simulations of Sarkar [4,3] for compressible homogeneous shear flow gives:

$$\beta = 0.025, \quad \lambda = 1.2$$

The present modification of the LRR model is also applied to the simulation of compressible mixing layers.

The homogeneous shear flow is closely related to the mixing layer [4]. Fig. 1 shows the variation of the gradient Mach number with the convective Mach number. This allows M_g to be connected to M_c as in Pantano and Sarkar [7], and the modified coefficient C_2 model becomes:

$$C_2 = C_2^I (1 + \lambda M_t^4) e^{(-\beta_1 M_c)} \quad (36)$$

The calibration of the coefficient λ_1 and β_1 based on the experiments of Goebel and Dutton [10] gives:

$$\lambda = 1.2, \quad \beta_1 = 0.055 \quad (37)$$

Turbulence models for the dilatational part of the turbulent dissipation and the correlation pressure-dilatation are needed. For these terms, we chose the models proposed by Sarkar et al. [2,15], namely:

$$\varepsilon_c = 0.5M_t^2 \varepsilon_s \quad (38)$$

$$\overline{p'd'} = \alpha_1 M_t \bar{\rho} \left(R_{ij} - \frac{2}{3} K \delta_{ij} \right) \tilde{U}_{i,j} + \alpha_2 \bar{\rho} M_t^2 \varepsilon_s + \alpha_3 M_t^2 \bar{\rho} k \tilde{U}_{i,i} \quad (39)$$

The model constants, α_1 , α_2 and α_3 , take the values: $\alpha_1 = 0.15$, $\alpha_2 = 0.2$, and $\alpha_3 = 0$.

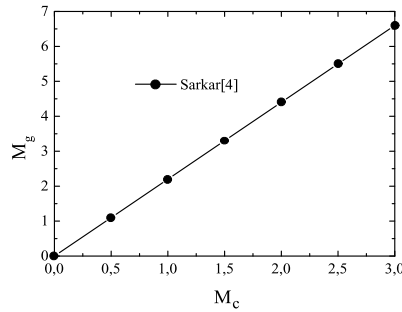


Fig. 1. Variation of the gradient Mach number with the convective Mach number.

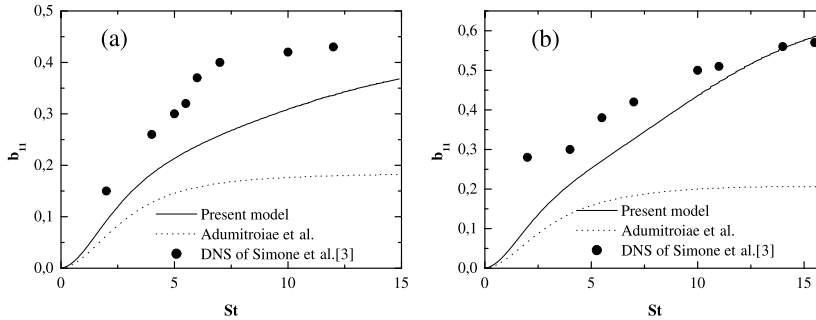


Fig. 2. Time evolution of the streamwise Reynolds stress anisotropy: b_{11} in cases (a) B_1 and (b) B_3 .

4. Applications of the proposed model

4.1. Simulation of compressible homogeneous shear flows

For compressible homogeneous shear flows, the mean velocity gradient is given by:

$$\tilde{U}_{i,j} = S\delta_{i1}\delta_{j2} \tag{40}$$

where S is the constant mean shear rate. Thus, the mean dilatation is:

$$\tilde{U}_{i,i} = 0 \tag{41}$$

$$\bar{\rho} = cte \tag{42}$$

The Favre averaged Reynolds stress should be a solution to the transport equation:

$$\bar{\rho} \frac{d}{dt} (\overline{u'_i u'_j}) = -(\overline{\rho u'_i u''_m} \tilde{U}_{j,m} + \overline{\rho u'_j u''_m} \tilde{U}_{i,m}) + \Phi_{ij}^* - \frac{2}{3} \bar{\rho} \varepsilon \delta_{ij} + \frac{2}{3} \overline{p' u'_{i,i} \delta_{ij}} \tag{43}$$

The turbulent kinetic energy and its dissipation rate are obtained by solving the following transport equations:

$$\bar{\rho} \frac{dk}{dt} = -\overline{\rho u'_i u''_j} \tilde{U}_{i,j} + \overline{p' u'_{i,i}} - \bar{\rho} \varepsilon \tag{44}$$

$$\bar{\rho} \frac{d\varepsilon_s}{dt} = -C_{\varepsilon 1} \bar{\rho} \frac{\varepsilon_s}{k} \overline{u'_i u''_j} \tilde{U}_{i,j} - C_{\varepsilon 2} \bar{\rho} \frac{\varepsilon_s^2}{k} \tag{45}$$

where $C_{\varepsilon 1}$ and $C_{\varepsilon 2}$ are respectively the model constants, $C_{\varepsilon 1} = 1.4$ and $C_{\varepsilon 2} = 1.9$.

The turbulent Mach number is described in [16] by the transport equation as follows:

$$\frac{DM_t}{Dt} = \frac{M_t}{2k} P + \frac{M_t}{2\bar{\rho}k} \left(1 + \frac{1}{2} \gamma (\gamma - 1) M_t^2 \right) (\overline{p'd'} - \bar{\rho} \varepsilon) \tag{46}$$

The ability of the proposed model for the pressure–strain correlation to predict characteristic properties of the compressible homogeneous turbulent shear flow will now be considered. The above averaged transport equations (43)–(46) are solved numerically for compressible homogeneous turbulence using a fourth-order Runge–Kutta numerical scheme. Figs. 2 to 9 show the proposed model predictions compared with those obtained with Adumitroaie et al.’s model [11] and with

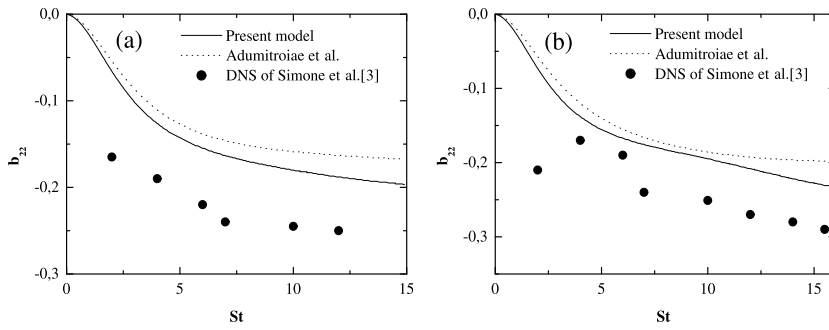


Fig. 3. Time evolution of the transverse Reynolds stress anisotropy: b_{22} in cases (a) B_1 and (b) B_3 .

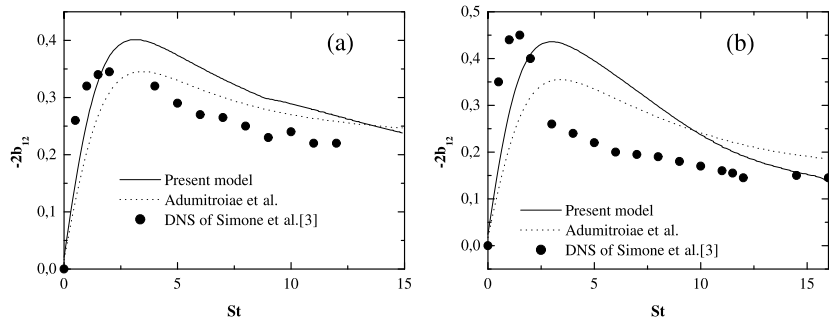


Fig. 4. Time evolution of the Reynolds shear-stress anisotropy: b_{12} in cases (a) B_1 and (b) B_3 .

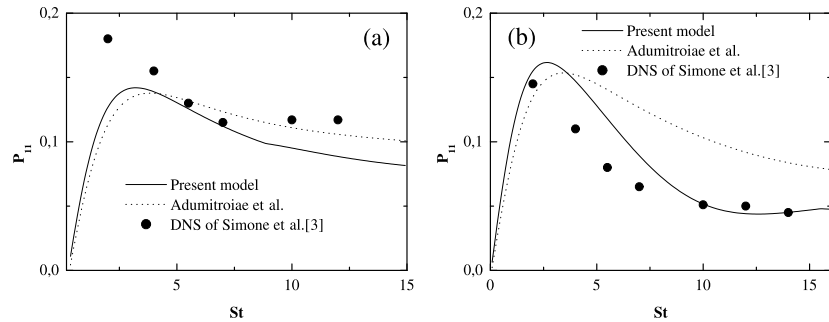


Fig. 5. Time evolution of the pressure strain: P_{11} in cases (a) B_1 and (b) B_3 .

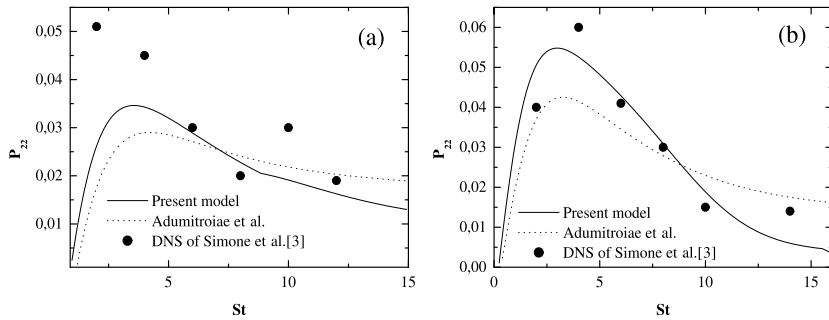


Fig. 6. Time evolution of the pressure strain: P_{22} in cases (a) B_1 and (b) B_3 .

the DNS results of Simone et al. [3] for cases B_1 and B_3 . Also, both models have been evaluated by using the DNS results of Sarkar [4]. In all these cases, DNS results correspond to the different initial conditions listed in Tables 1 and 2.

Figs. 2, 3 and 4 show the non-dimensional time (St) variation of the Reynolds stress anisotropies b_{11} , b_{22} , and b_{12} . From these figures, it is clear that the proposed model appears to be able to predict correctly the significant decrease in the normalized turbulent production term $-2b_{12}$ and the increase in the streamwise term b_{11} , as well as the transverse b_{22}

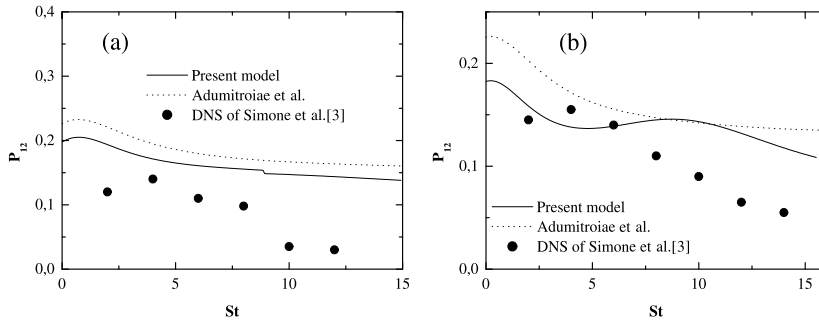


Fig. 7. Time evolution of the pressure strain: P_{12} in cases (a) B_1 and (b) B_3 .

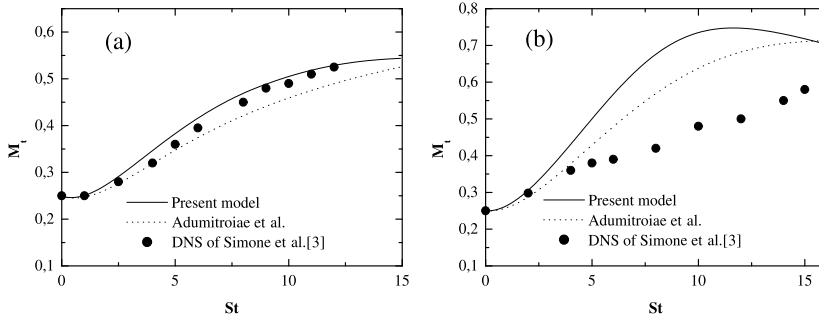


Fig. 8. Time evolution of the turbulent Mach number: M_t in cases (a) B_1 and (b) B_3 .

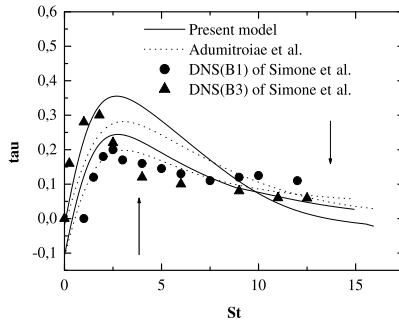


Fig. 9. Time evolution of the growth rate of the turbulent kinetic energy: $\tau = A$ in cases B_1 and B_3 . The arrows show the trend with increasing M_g values.

Table 1
Initial conditions for DNS [4] of homogeneous turbulent shear flow.

Case	M_{g0}	M_{t0}	$(Sk/\epsilon)_0$	b_{11}	b_{22}	b_{12}
A_1	0.22	0.4	1.8	0	0	0
A_2	0.44	0.4	3.6	0	0	0
A_3	0.66	0.4	5.4	0	0	0
A_4	1.32	0.4	10.8	0	0	0

Table 2
Initial conditions for DNS [3] of homogeneous turbulent shear flow.

Case	M_{g0}	M_{t0}	$(Sk/\epsilon)_0$	b_{11}	b_{22}	b_{12}
B_1	0.6	0.25	8	0	0	0
B_3	1.9	0.25	24	0	0	0

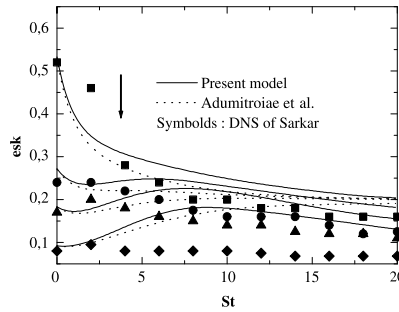


Fig. 10. Time evolution of the turbulent dissipation rate: $esk = \varepsilon_s/SK$ in cases $A_1, A_2, A_3,$ and A_4 . The arrow shows the trend with increasing M values.

Table 3

Comparison of the present model predictions for the long-time values of the anisotropy tensor for cases A_1 to A_4 and with the DNS results of Sarkar [4].

Cases	Adumitroiae et al.'s model [11]			Proposed model			DNS results of Sarkar		
	b_{11}	b_{22}	b_{12}	b_{11}	b_{22}	b_{12}	b_{11}	b_{22}	b_{12}
A_1	0.184	-0.145	-0.165	0.338	-0.169	-0.141	0.32	-0.2	-0.145
A_2	0.189	-0.147	-0.155	0.425	-0.182	-0.1025	0.44	-0.24	-0.12
A_3	0.197	-0.152	-0.148	0.49	-0.19	-0.09	0.51	-0.275	-0.092
A_4	0.214	-0.168	-0.142	0.62	-0.236	-0.058	0.6	-0.31	-0.06

Reynolds stresses anisotropies with increasing the gradient Mach number. Results obtained with Adumitroiae et al.'s model [11] disagree with DNS data, especially at high- M_g values; in case B_3 , this model is still unable to predict the changes in the magnitude of the Reynolds stress anisotropy when the compressibility is higher. Figs. 5, 6 and 7 present the behavior of the pressure-strain correlation $\Pi_{ij} = \varphi_{ij}^*/2SK$. As can be seen in these figures, the proposed model yields acceptable results that are in good qualitative agreement with the DNS data, especially at high gradient Mach number. The predicted results of the turbulent Mach number are plotted in Fig. 8. It can clearly be seen that both models appear to be able to predict the correct trend of the M_t - increase with increasing the initial values of M_g . The predicted results for the growth rate of the turbulent kinetic energy ($\Lambda = (dK/dt)/SK$) are shown in Fig. 9. It can clearly be seen that both models are able to predict accurately the trend towards a reduced growth rate with increasing the initial values of the gradient Mach number. This phenomenon has often been observed in DNS results of compressible homogeneous shear flows. For the initial time, Λ show a systematic increase from cases B_1 to B_3 . To find the cause of this discrepancy, an equation for Λ is written as follows [4,3]:

$$\Lambda = -2b_{12}(1 - \chi)$$

where $\chi = \frac{\varepsilon_s + \varepsilon_c - \overline{p'd'}}{SK}$, includes dilatational effects.

For initial times, $St \leq 5$, $-2b_{12}$ shows little difference between the different cases, as it is shown in Fig. 4. According to DNS results [4,3], it is easy to see that the difference between the values of $-2b_{12}$ is much smaller than that between χ values for initial times for cases B_1 to B_3 . We notice that $\chi_d = \frac{\varepsilon_c - \overline{p'd'}}{SK}$ is much larger in case B_3 compared to that in case B_1 . This implies that the important increase in magnitude of χ is the principal cause for the increase in the initial-time values of Λ . On the contrary, for $St \geq 12$, χ_d becomes much smaller and the reduction of $-2b_{12}$ is responsible for the lowered growth rate of the turbulent kinetic energy.

Fig. 10 present the behavior of the normalized dissipation (ε_s/SK) for cases A_1, A_2, A_3 and A_4 from DNS inferred from DNS results [4]. It can be seen that there is a decrease in ε_s/SK when M_{g0} increases, since the compressibility effects cause significant reduction in the production from numerical simulation cases A_1 to A_4 . All models are in acceptable accordance with the DNS results of Sarkar [4]. From the above figures, one can remark that, particularly at high compressibility values (case B_3), there are substantial differences between the two models in their predictions. This can be found in the different ways on which these models are developed. The model of Adumitroiae et al. [11] is based on a modeling approach similar to that used for the incompressible flows. Probably, this can explain the observed deficiency of this model in the prediction of the high-speed shear flow.

It is relevant to note that for $St = 20$ the turbulence seems to evolve towards equilibrium states. This can be seen more clearly in Table 3 that shows a systematic comparison between the models predictions for the long-time values of b_{ij} and the DNS results of Sarkar [4].

From Table 3, one can see that for high compressibilities, the proposed model is much better to predict accurately the equilibrium values of b_{ij} for compressible shear flows than Adumitroiae et al.'s one.

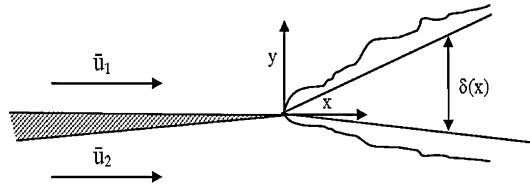


Fig. 11. The compressible mixing layers.

Table 4
Initial conditions for experiments results [10] of mixing layers.

M_c	$r = \frac{U_2}{U_1}$	$s = \frac{\rho_2}{\rho_1}$
0.2	0.78	0.76
0.46	0.57	1.55
0.69	0.18	0.57
0.86	0.16	0.6
1.0	0.16	1.14

4.2. Simulation of the compressible mixing layer

Now we choose to examine the performance of the proposed model for the pressure–strain correlations (see Section 3) in simulating fully developed stationary compressible mixing layers. The flow is governed by the averaged Navier–Stokes equations associated with those describing energy, Reynolds stress, and turbulent dissipation. The simplest of the resulting continuity, momentum and energy equations for stationary mixing layers can be written as:

$$\frac{\partial}{\partial x_i}(\bar{\rho}\tilde{U}_i) = 0 \tag{47}$$

$$\frac{\partial}{\partial x_j}(\bar{\rho}\tilde{U}_i\tilde{U}_j) = -\frac{\partial}{\partial x_j}(\overline{\rho u_i'' u_j''}) \tag{48}$$

$$\frac{\partial}{\partial x_i}(\bar{\rho}\tilde{C}_v\tilde{T}\tilde{U}_i) = -p' \frac{\partial}{\partial x_i} u_i'' + \varepsilon_c + \varepsilon_s - \frac{\partial}{\partial x_i} \bar{\rho} C_v \overline{u_i'' T''} \tag{49}$$

The Reynolds stress equation is written

$$\frac{\partial}{\partial x_m}(\bar{\rho}\overline{u_i'' u_j'' \tilde{U}_m}) = -(\bar{\rho}\overline{u_i'' u_m'' \tilde{U}_{j,m}} + \bar{\rho}\overline{u_j'' u_m'' \tilde{U}_{i,m}}) - (\bar{\rho}\overline{u_i'' u_j'' u_m''})_{,m} + \phi_{ij}^* + \frac{2}{3}\overline{p'd'}\delta_{ij} - \frac{2}{3}\varepsilon\delta_{ij} \tag{50}$$

The solenoidal dissipation rate shall be calculated using the classical model equation:

$$\frac{\partial}{\partial x_k}(\bar{\rho}\tilde{U}_k\varepsilon_s) = \frac{\varepsilon_s}{K} \left(C_{\varepsilon_1} \bar{\rho}\overline{u_k'' u_m''} \frac{\partial}{\partial x_m} \tilde{U}_k - \bar{\rho} C_{\varepsilon_2} \varepsilon_s \right) + \frac{\partial}{\partial x_k} \left(-C_{\varepsilon_3} \bar{\rho} \frac{K}{\varepsilon} \overline{u_k'' u_m''} \frac{\partial}{\partial x_m} \varepsilon_s \right) \tag{51}$$

In the above-mentioned transport equations, several terms should be modeled. The gradient diffusion hypothesis is used to model:

- the turbulent heat flux [17]

$$\overline{u_i'' T''} = -C_t \frac{K}{\varepsilon} \overline{u_i'' u_m''} \frac{\partial}{\partial x_m} \tilde{T} \tag{52}$$

- the diffusion term [17]

$$\overline{u_i u_j u_m} = -C_s \frac{K}{\varepsilon} \overline{u_k'' u_m''} \frac{\partial}{\partial x_m} \overline{u_k'' u_m''} \tag{53}$$

The basic equations (47) to (51) on which the second-order closure for the stationary compressible mixing layers is based are solved using a finite-difference scheme. We have calculated two free streams (see Fig. 11), characterized typically by M_c and respectively by the ratios of the density $s = \frac{\rho_2}{\rho_1}$ and the velocity $r = \frac{U_2}{U_1}$.

The inlet free stream conditions are those corresponding to the experiments of Goebel and Dutton [10] as mentioned in Table 4.

The values of the constants used in the following simulation are:

$$C_{\varepsilon_1} = 1.4, \quad C_{\varepsilon_2} = 1.8, \quad C_{\mu} = 0.09, \quad C_{\varepsilon_3} = 0.18, \quad C_s = 0.26, \quad C_t = 0.25$$

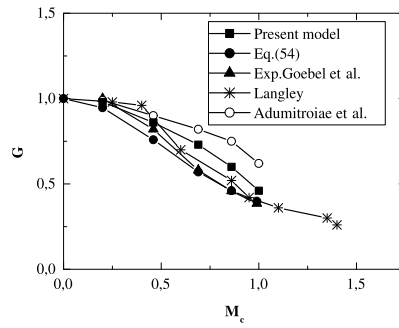


Fig. 12. Normalized growth rate G versus convective Mach number M_c .

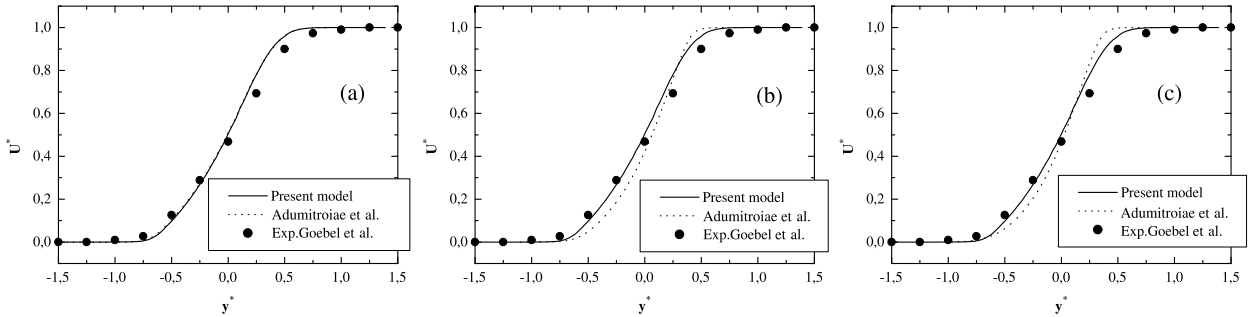


Fig. 13. Similarity profiles of the mean velocity in two-stream mixing layers: (a) $M_c = 0.46$, (b) $M_c = 0.69$, (c) $M_c = 0.86$.

The proposed model’s predictions will be compared with those obtained by Adumitroaie et al.’s model [11], and the experimental results of Goebel and Dutton [10] for different values of the convective Mach number. The fundamental parameter characterizing the effects of compressibility on the compressible mixing layers is the growth rate $(\frac{d\delta}{dx})$, where δ denotes the momentum thickness of the mixing layer. The width of δ is defined by the transverse distance between the two positions where the non-dimensional velocity $U^* = \frac{U-U_2}{U_1-U_2}$ equals 0.1 and 0.9. Fig. 12 shows the comparison between the computed normalized growth rate by its value in the incompressible case, $G = (\frac{d\delta}{dx}) / (\frac{d\delta}{dx})_{M_c=0}$ with different experimental results available in the literature and with those obtained by the empirical formula of Dimotakis [18]:

$$G = 0.8e^{(-M_c^2)} + 0.2 \tag{54}$$

The growth rate G predicted by the proposed model decreases with increasing the convective Mach number, in agreement with experimental results. This phenomenon that is observed in experimental studies of compressible mixing layers is over-predicted by the model of Adumitroaie et al. [11], the reduction of G with M_c is slightly smaller than in the experimental results [10]. The normalized stream mean velocity U^* is represented in relation to the similarity variable $y^+ = (y - y_c) / \delta$ in Fig. 13, where y is the local cross-stream coordinate and y_c is the cross-stream coordinate corresponding to $U^* = 0.5$. The velocity profiles calculated through the two models are in reasonable agreement with the experimental results [10]. The effects of the two Mach numbers M_t and M_c on the changes in the pressure–strain correlation are clearly seen in Figs. 14, 15 and 16, which respectively compare the similarity profiles of the streamwise $R_{11} = \widetilde{u''^2} / (U_1 - U_2)^2$, the transverse $R_{22} = \widetilde{v''^2} / (U_1 - U_2)^2$ and the shear stress $R_{12} = \widetilde{u''v''} / (U_1 - U_2)^2$ turbulence intensities of the Reynolds stress obtained by the proposed model and Adumitroaie et al.’s one [11] with the experimental results [10] for three values of the convective Mach number. Examination of these figures indicates that the proposed model’s predictions of these turbulent quantities are in good agreement with the experimental results [10]. One can see that the peak values predicted by the proposed model are closer to the experimental peaks [10] than those predicted by Adumitroaie et al.’s model, this latter model underestimating $(R_{11})_{max}$ and overpredicts $(R_{22})_{max}$ and $((-R_{12})^{1/2})_{max}$. However, all these turbulence quantities appear to be accurately captured by the proposed model.

The current study shows that the changes in the structural compressibility effects of the pressure–strain correlation are key to explain the observed behaviors. The convective Mach number seems to be an adequate parameter for characterizing such effects on mixing layers.

5. Conclusion

In this study, the widely known second-order closure has been used for the prediction of compressible turbulent shear flows. The standard Reynolds stress turbulence closure with the addition of the pressure–dilatation and compressible dis-

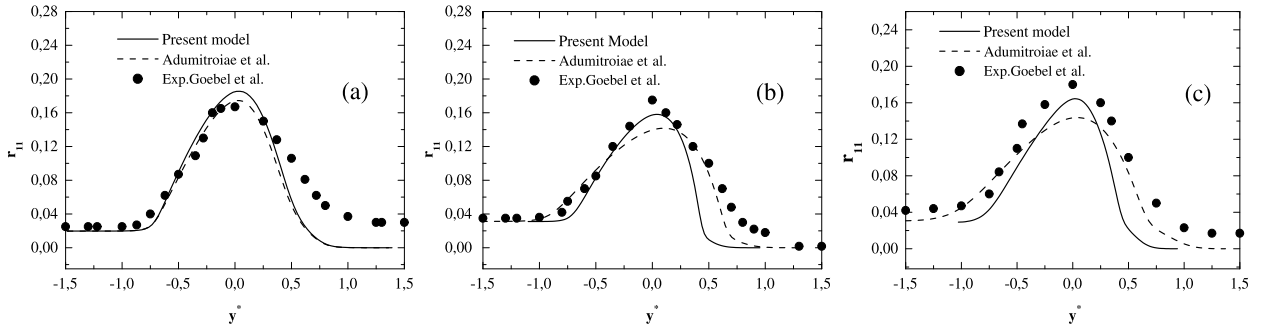


Fig. 14. Similarity profiles of longitudinal turbulence intensity: (a) $M_c = 0.46$, (b) $M_c = 0.69$, (c) $M_c = 0.86$.

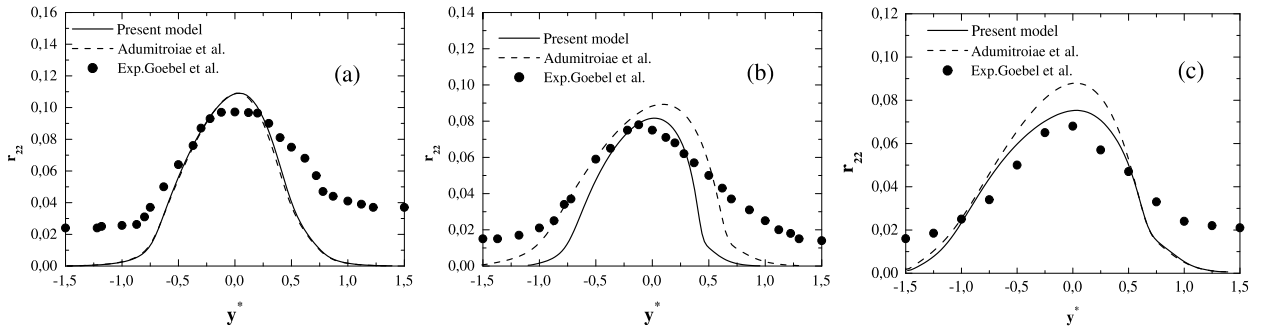


Fig. 15. Similarity profiles of transverse turbulence intensity: (a) $M_c = 0.46$, (b) $M_c = 0.69$, (c) $M_c = 0.86$.

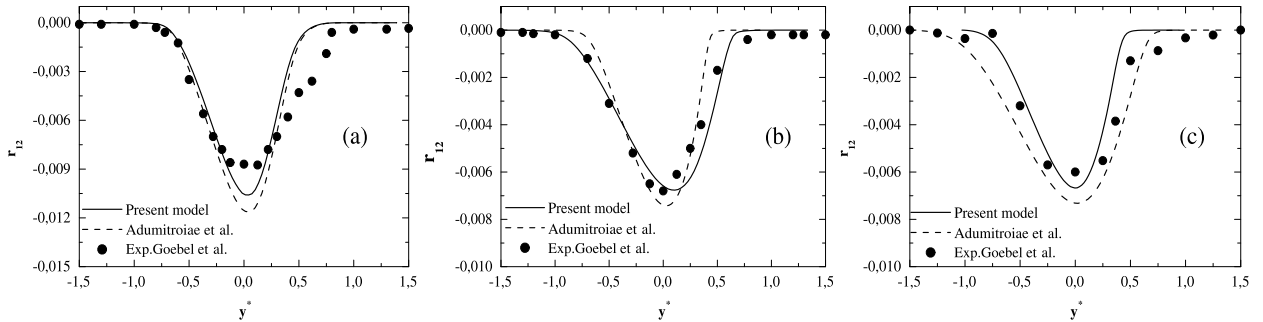


Fig. 16. Similarity profiles of shear turbulence intensity: (a) $M_c = 0.46$, (b) $M_c = 0.69$, (c) $M_c = 0.86$.

sipation models yields very poor predictions of the changes in the Reynolds-stress anisotropy magnitude. The deficiency of this closure is due to the use of the incompressible models of the pressure–strain correlation. A new version of the extended LRR model [8] involving the gradient Mach numbers M_g and M_c with the commonly used the turbulent Mach number M_t has been proposed to reflect compressibility effects. A comparison has been made between the behaviors of the proposed model and the compressible model of Adumitroaie et al. [11] for the pressure–strain correlation in two different applications: the compressible homogeneous shear flow and the mixing layers. The proposed model shows satisfactory agreement with available DNS [4,3] and experimental results [10]. This model appears to be able to predict accurately the structural compressibility effects: the significant decrease in the magnitude of the Reynolds shear stress, the increase in magnitude of the diagonal components of the Reynolds stress anisotropies with increasing initial values of the gradient Mach number. Also, the asymptotic states of the flow are well predicted by the proposed model, and the equilibrium values of the Reynolds stress anisotropies are in accordance with the DNS data. In compressible mixing layer flows, the proposed model successfully predict the reduced growth rate and the decrease in the Reynolds stress peaks with increasing the convective Mach number. Also, the similarity velocity is well predicted by the proposed model. The model of Adumitroaie et al. [11] predicts satisfactorily the behaviors of the compressible homogeneous shear flow and the mixing layers at low compressibility values, but fails to predict high structural compressibility effects on these flows. Therefore, the gradient Mach numbers M_g and M_c are found out to be important parameters in addition to M_t in the modeling of the pressure–strain correlation with respect to turbulent compressible homogeneous shear flows and mixing layers.

References

- [1] O. Zeman, Dilatation dissipation, the concept and application in modeling compressible mixing layers, *Phys. Fluids A* 2 (1990) 178.
- [2] S. Sarkar, G. Erlebacher, M.Y. Hussaini, H.O. Kreiss, The analysis and modeling of dilatational terms in compressible turbulence, *J. Fluid Mech.* 227 (1991) 473.
- [3] A. Simone, G.N. Coleman, C. Cambon, The effect of compressibility on turbulent shear flow: a rapid distortion-theory and direct numerical simulation study, *J. Fluid Mech.* 330 (1997) 307–338.
- [4] S. Sarkar, The stabilizing effects of compressibility in turbulent shear flow, *J. Fluid Mech.* 282 (1995) 163.
- [5] F. Hamba, Effects of pressure fluctuations on turbulence growth compressible homogeneous shear flow, *Phys. Fluids A* 6 (1999) 1625.
- [6] A.W. Vreman, N.D. Sandham, K.H. Luo, Compressible mixing layer growth rate and turbulence characteristics, *J. Fluid Mech.* (1996) 320–325.
- [7] C. Pantano, S. Sarkar, A study of compressibility effects in the high-speed turbulent shear layer using direct simulation, *J. Fluid Mech.* 451 (2002) 329–371.
- [8] H. Marzougui, H. Klifi, T. Lili, Extension of the Launder, Reece and Rodi on compressible homogeneous shear flow, *Eur. Phys. J. B* 45 (2005) 147–154.
- [9] B.E. Launder, G.J. Reece, W. Rodi, Progress in the development of a Reynolds-stress turbulence closure, *J. Fluid Mech.* 68 (1975) 537.
- [10] S.G. Goebel, J.C. Dutton, Experimental study of compressible turbulent mixing layers, *AIAA J.* 29 (1981) 538.
- [11] V. Adumitroaie, J.R. Risorcelli, D.B. Taulbee, Progress in Favre Reynolds stress closures for compressible flows, *Phys. Fluids A* 9 (1999) 2696.
- [12] C.H. Park, S.O. Park, A compressible turbulence model for the pressure–strain correlation, *J. Turbul.* 6 (2) (2005) 1–25.
- [13] H. Fujiwara, C. Arakawa, Modeling of compressible turbulent flows with emphasis on pressure–dilatation correlation, *Eng. Turbulence Model. Exp.* 3 (1996) 151.
- [14] S. Heinz, *Statistical Mechanics of Turbulent Flows*, Springer Verlag, Berlin, 2003.
- [15] S. Sarkar, The pressure–dilatation correlation in compressible flows, *Phys. Fluids A* 4 (1992) 2674.
- [16] C.G. Speziale, R. Abid, N. Mansour, Evaluation of Reynolds-stress turbulence closures in compressible homogeneous shear flow, *ZAMPS* 17 (1985).
- [17] C.G. Speziale, S. Sarkar, Second-order closure models for supersonic turbulent flows, NASA Langley Research Center, Hampton, ICASE Report 91-9, 1991.
- [18] P.E. Dimotakis, Turbulent free shear layer mixing and combustion, in: S.N.B. Murthy, E.T. Curran (Eds.), *Progress in Astronautics and Aeronautics*, vol. 137, AIAA, Washington, DC, 1991.